Electronic Supplementary Material (ESI) for ChemComm.

Photocatalytic multiphase micro-droplet reactors based on complex coacervation

Kangle Lv,[a] Adam W. Perriman,*[b,c] Stephen Mann*[c]

[a] Key Laboratory of Catalysis and Materials Science of the State Ethnic Affairs Commission & Ministry of Education, South-Central University for Nationalities, Wuhan 430074, China.

[b] School of Cellular and Molecular Medicine, University of Bristol, BS8 1TD, United Kingdom.

[c] Centre for Organized Matter Chemistry and Centre for Protolife Research, School of Chemistry, University of Bristol, BS8 1TS, United Kingdom.

Supporting Information

METHODS

Preparation and characterisation of photocatalytic coacervate droplets

All chemicals were purchased from Sigma-Aldrich and used without further purification. All aqueous solutions were prepared using Milli-Q quality (18.2 MΩ·cm) water. Turbid coacervate micro-droplet dispersions (pH 7-8) were produced by adding 600 μL of a 50 mM poly(diallyldimethylammonium) chloride (PDDA, Mw 100–200 kDa) solution to either 200 μL of 50 mM adenosine $5^{/}$-triphosphate (ATP) or 50 mM poly(ethylene glycol) 4-nonylphenyl 3-sulfopropyl ether potassium salt (KPSE, Mw 1.2 kDa). For TiO_2 nanosheet-containing coacervate droplets, 4 mg of TiO_2 nanosheets (TiO_2NS) prepared as described previously[7] was dispersed in the PDDA stock solution to give a concentration of 0.67 mg mL^{-1}, before addition to the respective ATP or KPSE solutions. TiO_2NS partition coefficient measurements were undertaken by separating the droplets from the aqueous suspensions by centrifugation at 5,000 rpm for 15 min to produce a bulk coacervate phase. After 12 h, the aqueous phase was removed, and the coacervate phase destabilised (0.5 M NaCl) to give a clear solution. The TiO_2NS partition coefficients were evaluated using UV-vis spectroscopy by comparing the ratio of the aqueous and bulk coacervate phase absorbances at 325 nm. Dynamic light scattering (DLS) and zeta potential measurements of the coacervate droplet and aqueous TiO_2 nanosheets dispersions were performed on a Malvern Zetasizer Nano-ZS. TiO_2 nanosheets were dispersed using sonication and measured at 0.5 and 0.01 mg mL^{-1} in water, and in 2.5 mM KPSE, ATP and PDDA.

Determination of dye partition coefficients.

Stock solutions of Methylene Blue (MB, 0.5 mg mL^{-1}, Abs_{max} = 668 nm), Rhodamine B (RhB, 0.5 mg mL^{-1}, Abs_{max} = 555 nm), Brilliant Red X-3B (X3B, 5 mg mL^{-1}, Abs_{max} = 510 nm) and Sulforhodamine B (SRhB, 0.5 mg mL^{-1}, Abs_{max} = 565 nm) were produced using Milli-Q quality (18.2 MΩ·cm) water. 10 μL of a stock dye solution was mixed with 600 μL of PDDA, followed by the addition of 200 μL of ATP or KPSE. The turbid coacervate droplet dispersions were shaken by hand for 2 min, sonicated for another 5 min, and then centrifuged at 5000 rpm for 5 min. Fluorophore absorption in the aqueous solution (upper layer, A1) was monitored directly using UV-vis spectroscopy, while fluorophore partitioning in the coacervate phase (lower layer, A2) was ascertained after decomposition using NaCl solution (10 μL in 990 μL 0.5 M NaCl). The partition coefficient of the dye (K) in the coacervate was determined as K = A2/A1 x dilution factor.

Photocatalytic studies

Photocatalytic dye degradation assays were performed by mixing 100 μL of a stock solution of Methylene Blue (MB, 0.5 mg mL^{-1}, Abs_{max} = 668 nm), Rhodamine B (RhB, 0.5 mg mL^{-1}, Abs_{max} = 555 nm), Brilliant Red X-3B (X3B, 5 mg mL^{-1}, Abs_{max} = 510 nm) or Sulforhodamine B (SRhB, 0.5 mg mL^{-1}, Abs_{max} = 565 nm) in Milli-Q quality (18.2 MΩ·cm) water with 8 mL of a stirred recipient solution followed by exposure to a LED lamp (365 nm ± 10 nm at 3 W). At given time intervals, 800 μL aliquots were removed from the solution and analysed using UV-vis spectroscopy. Photocatalytic dye degradation experiments were performed on each of the four dyes in TiO_2NS/PDDA/ATP and TiO_2NS/PDDA/KPSE coacervate droplet dispersions, and in the pure coacervate phases. Selective dye degradation using RhB and MB assays were performed in TiO_2NS/PDDA/ATP/ coacervate droplet dispersions. Where necessary, 10 or 30 μL of 5 M NaCl was added to destabilise the PDDA/ATP or PDDA/KPSE coacervate droplet dispersions respectively. TiO_2 nanosheets were also removed by centrifugation (10000 rpm for 5 min) before UV-vis spectroscopy analyses. Control degradation experiments involving the dyes in the presence of each constituent component in isolation were also performed. Exponential decay constants (λ) were evaluated by fitting an exponential decay curve to the time-dependent normalised dye-degradation UV-vis spectroscopy data.

Synthesis and characterisation of TiO_2 (anatase) nanosheets.

8 mL of a HF solution (40 wt.%, 20.0 mol L^{-1}) was added dropwise to 50 g of tetrabutyltitanate (TBT) and the solution stirred for 5 min. The solution was then transferred to a dry PTFE-lined autoclave (100 mL) and kept at 200°C for 24 h. The resulting precipitate was filtered (0.45 μm), washed with Milli-Q quality (18.2 MΩ·cm) water, and dried in a vacuum oven at 80°C for 10 h. The morphology of the photocatalyst was observed on a transmission electron microscopy (TEM) (Tecnai G20, USA) using an acceleration voltage of 200 kV. Typically, a small aliquot of the aqueous TiO_2 nanosheets sample was allowed to adsorb for 2 minutes onto carbon-coated copper grids and the excess was then wicked away before air-drying.

Simulation of the lipophilic partition coefficient contributions

The theoretical lipophilic partition coefficient (log*D*) values were calculated using the physico-chemical property predictor plugin in MarvinSketch (14.12.15.0) (ChemAxon). The approach is based on a modified version of the method described previously [V. N. Viswanadhan, A. K. Ghose, G. R. Revankar, R. K. Robins, *J. Chem. Inf. Comput. Sci.* **1989**, 29, 163-172]. Briefly, the predicted partition coefficient was evaluated using the molecules' atomic increments where the calculation included the redefinition of selected atom types to accommodate electron delocalization, as well as the addition of contributions from ionic species. As log *D* values are dependent on pH, the calculations were dependent on estimates of the *p*Ka of the ionisable groups. A sodium chloride concentration of 2 mM was used for all calculations, which corresponded to the counterions associated with the coacervate constituents.

SI FIGURES

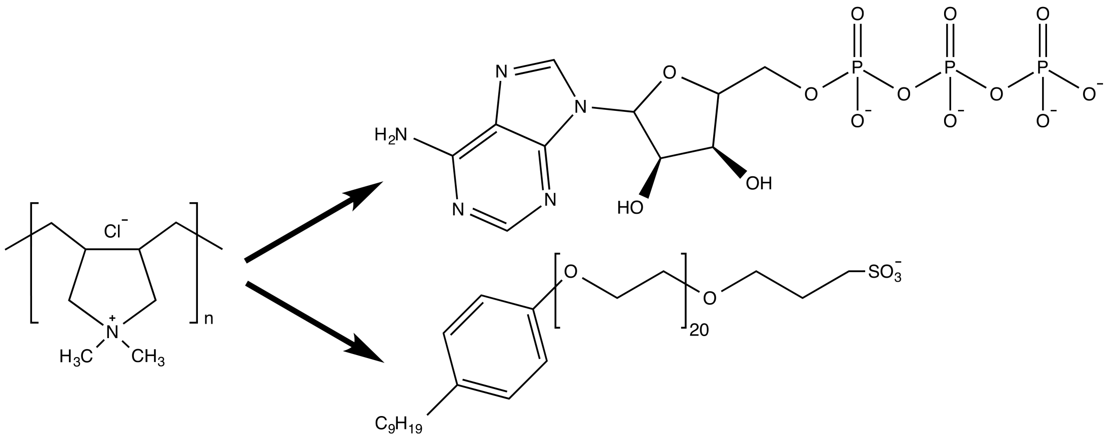

Figure S1. Scheme showing molecular components used to prepare coacervate micro-droplets by addition of poly(diallyldimethylammonium) chloride (PDDA) to either **(i)** adenosine triphosphate (ATP) or **(ii)** poly(ethylene glycol) 4-nonylphenyl 3-sulfopropyl ether (KPSE).

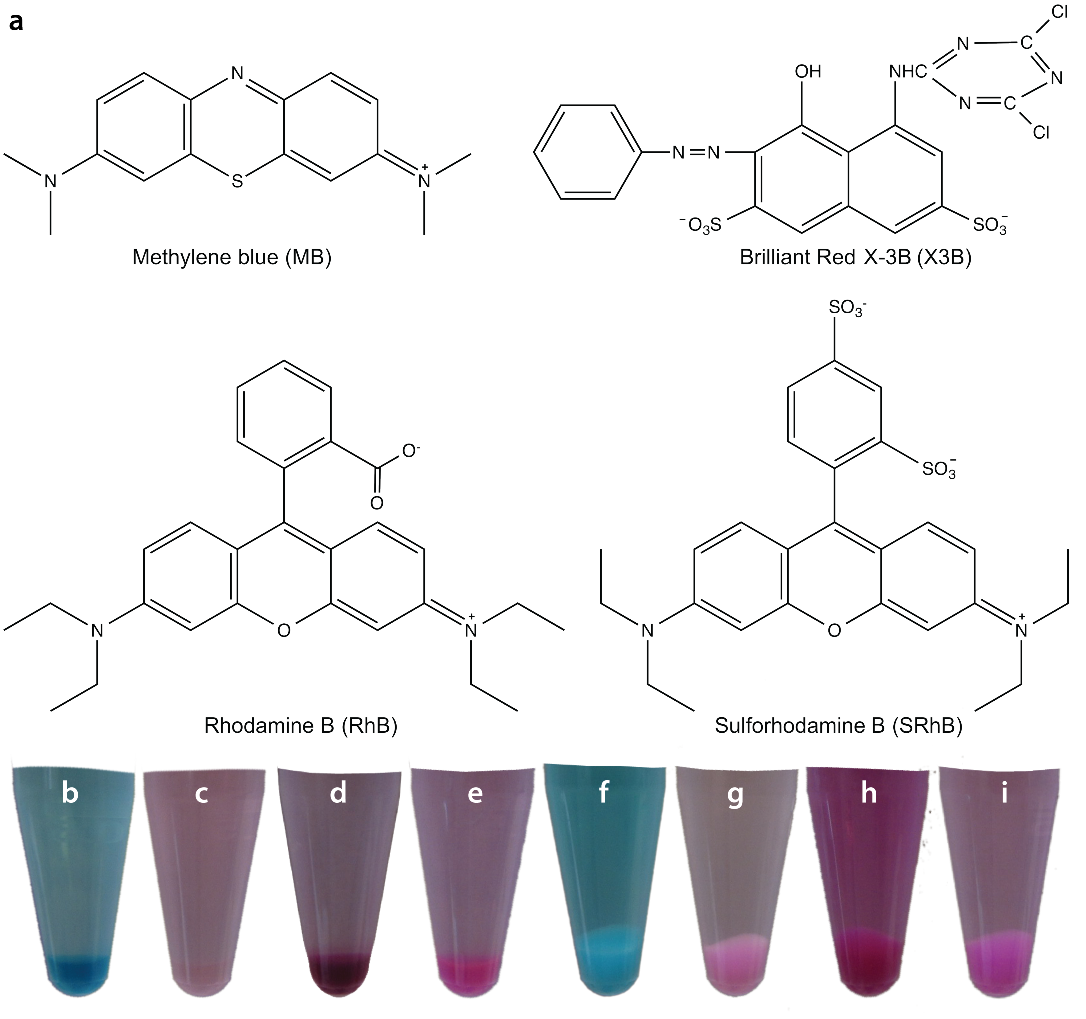

Figure S2. (a) Dye chemical structures. (b-i) Photographs showing partitioning of the dyes between the upper aqueous continuous phase and lower coacervate phase after centrifugation of PDDA/ATP droplet dispersions containing **(b)** Methylene Blue (MB), **(c)** Rhodamine B (RhB), **(d)** Brilliant Red X-3B (X3B), **(e)** Sulforhodamine B (SRhB); and PDDA/KPSE droplet dispersions containing **(f)** MB, **(g)** RhB, **(h)** X3B, **(i)** SRhB.

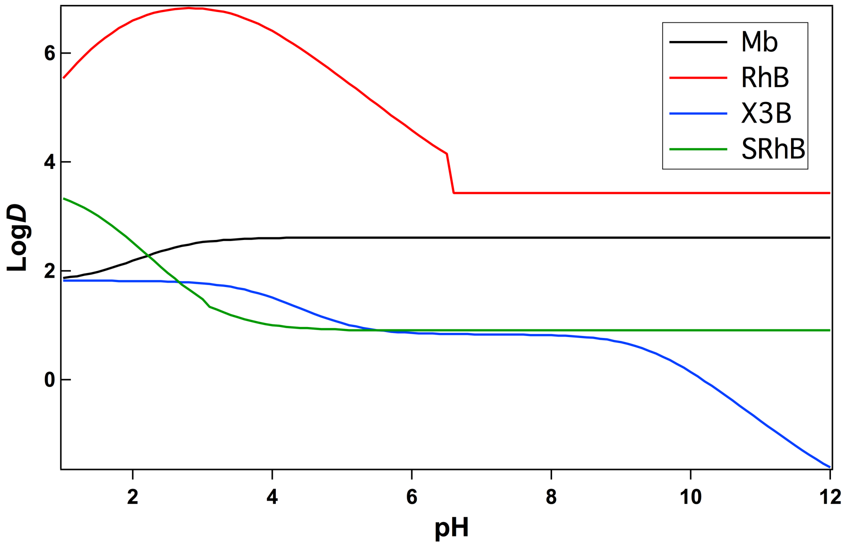

Figure S3. Simulations of the partition coefficients (log*D*) as a function of pH for Methylene Blue (MB, black line), Rhodamine B (RhB, red line), Brilliant Red X-3B (X3B, blue line), and Sulforhodamine B (SRhB, green line). Acid/base dissociation coefficients were used to generate the partition coefficient contributions from cationic, anionic and neutral species.

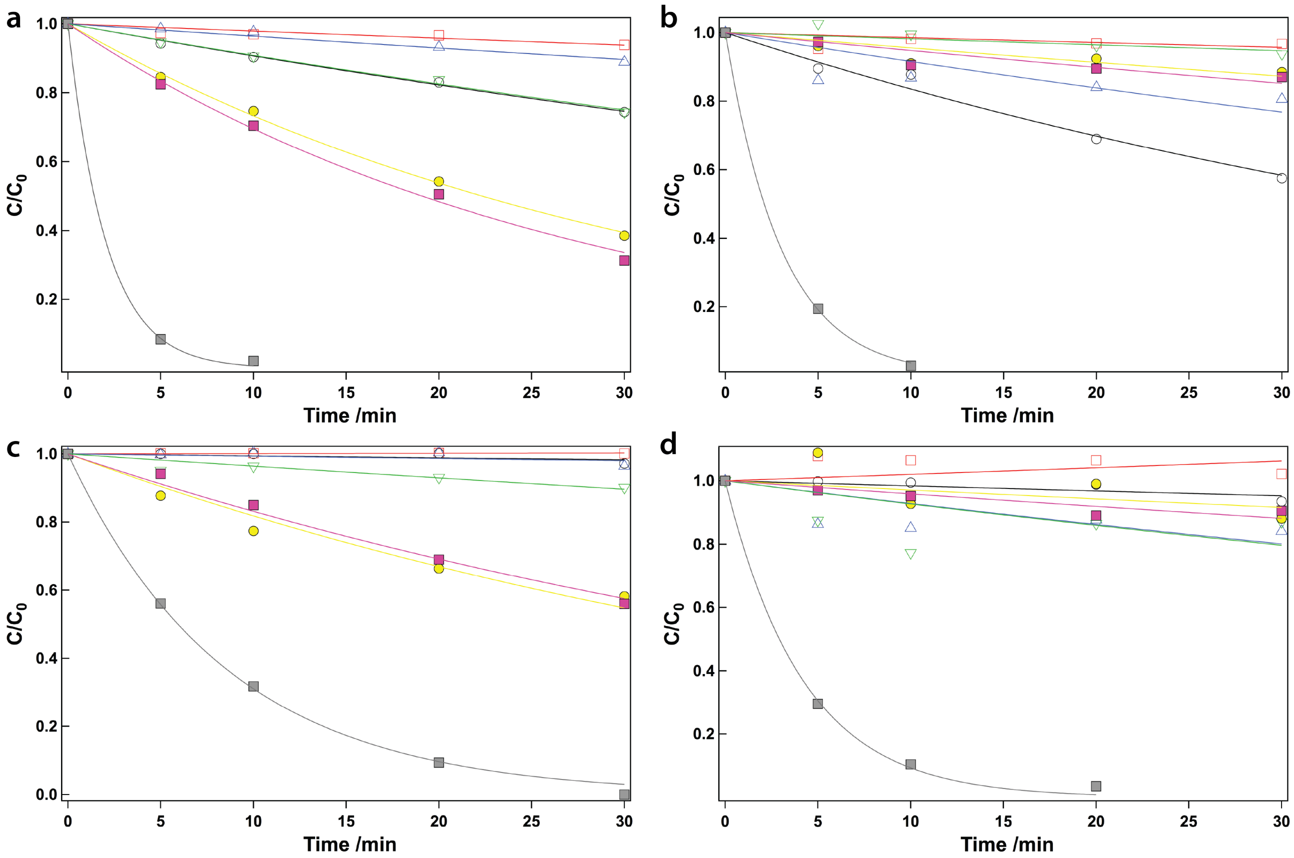

Figure S4. Full data set for photocatalytically induced dye degradation in TiO_2NS/PDDA/ATP coacervate micro-droplets on exposure to UV radiation (365 nm ± 10 nm @ 3 W). Plots show the time-dependent reduction in the normalized dye concentration for **(a)** Methylene Blue (MB), **(b)** Rhodamine B (RhB), **(c)** Brilliant Red X-3B (X3B), and **(d)** Sulforhodamine B (SRhB) in water (black, open circles), 37.5 mM PDDA (red, open squares), 12.5 mM ATP (blue, open triangles), PDDA/ATP coacervate micro-droplets (green, inverted open triangle), TiO_2NS/PDDA/ATP coacervate micro-droplets (yellow, solid circles), TiO_2NS/PDDA/ATP coacervate micro-droplets after addition of 5 M NaCl (purple, solid squares), and TiO_2NS in water (grey line, solid squares).

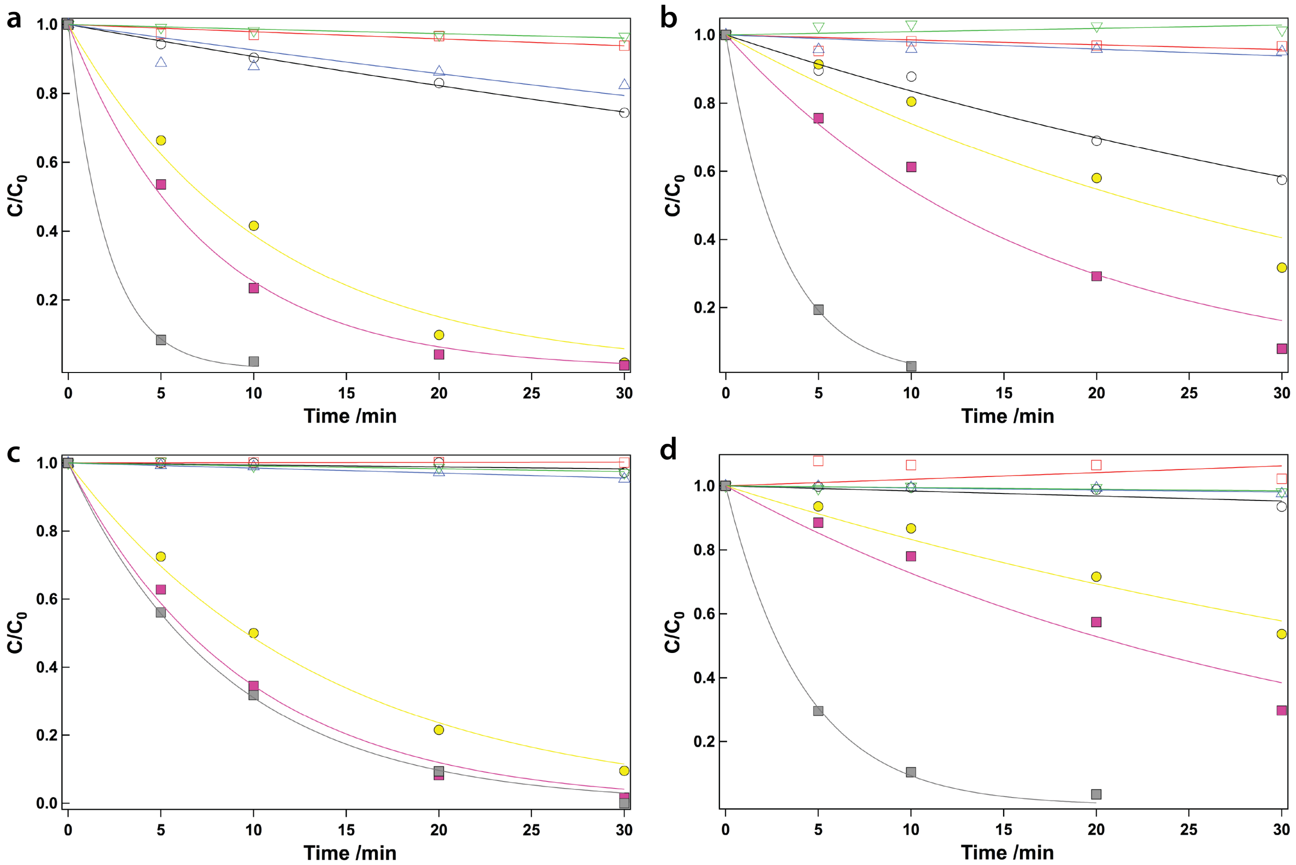

Figure S5. Full data set for photocatalytically induced dye degradation in TiO$_2$NS/PDDA/KPSE coacervate micro-droplets on exposure to UV radiation (365 nm ± 10 nm @ 3 W). Plots show the time-dependent reduction in the normalized dye concentration for **(a)** Methylene Blue (MB), **(b)** Rhodamine B (RhB), **(c)** Brilliant Red X-3B (X3B), and **(d)** Sulforhodamine B (SRhB) in water (black, open circles), 37.5 mM PDDA (red, open squares), 12.5 mM KPSE (blue, open triangles), PDDA/KPSE coacervate micro-droplets (green, inverted open triangle), TiO$_2$NS/PDDA/KPSE coacervate micro-droplets (yellow, solid circles), TiO$_2$NS/PDDA/KPSE coacervate micro-droplets after addition of 5 M NaCl (purple, solid squares), and TiO$_2$NS in water (grey line, solid squares).

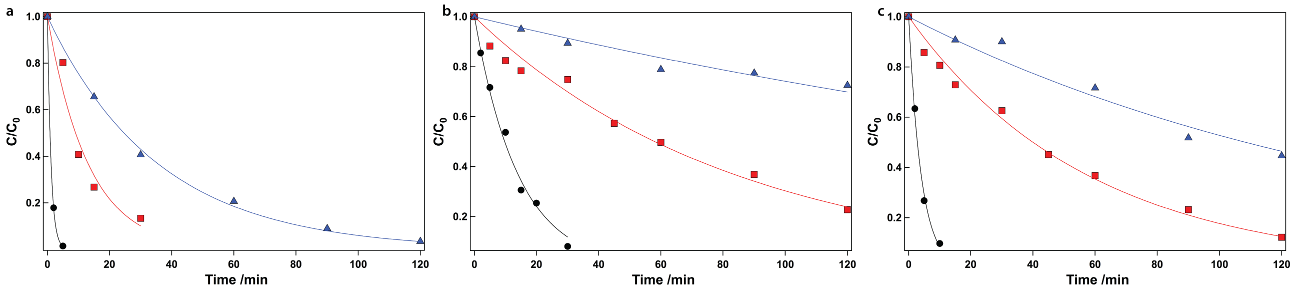

Figure S6. Plots showing time-dependent decrease in normalized MB concentrations associated with UV-photocatalytic degradation for **(a)** dispersion of TiO$_2$NS in water, **(b)** TiO$_2$NS/PDDA/KPSE bulk coacervate phase, and **(c)** TiO$_2$NS/PDDA/KPSE coacervate micro-droplets. In each case, the TiO$_2$NS final concentrations were 2.5 mg mL^{-1} (black circles), 0.125 mg mL^{-1} (red squares) or 0.05 mg mL^{-1} (blue triangles).

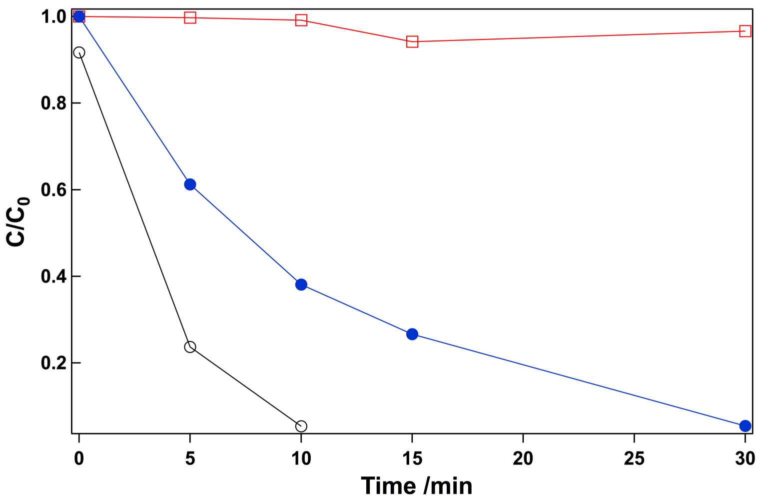

Figure S7. Photocatalytic degradation of SRhB in aqueous solution containing TiO_2NS only (black line and open circle), TiO_2NS and ATP (red line and open squares) or TiO_2NS and PDDA (blue line, filled circles).

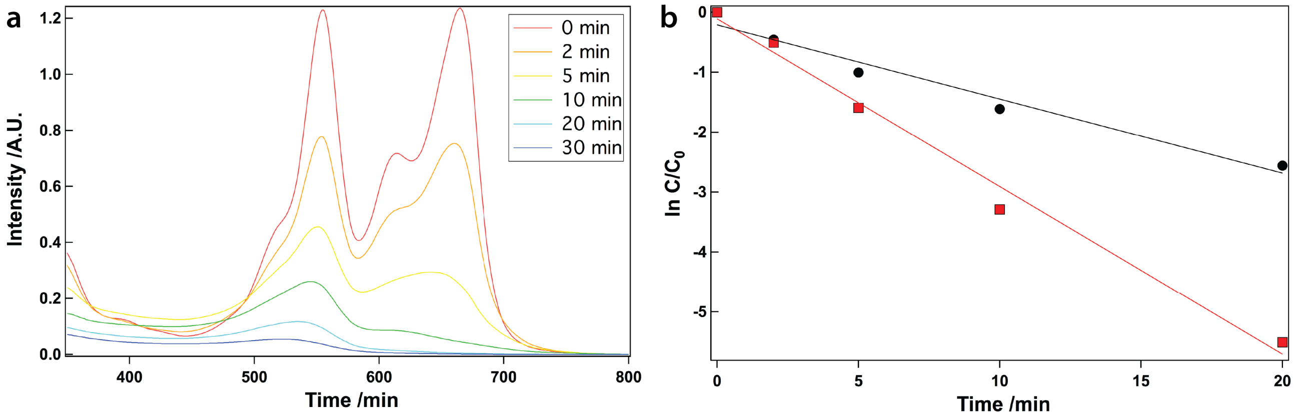

Figure S8. Selective dye degradation in photocatalytic TiO_2NS dispersed in water. (**a**) UV-vis spectra showing time-dependent changes in the intensity of the spectral features from a mixed solution of Methylene Blue (MB; abs$_{max}$ = 668 nm) and Rhodamine B (RhB; abs$_{max}$ = 555 nm). (**b**) Plots of time-dependent changes in the natural logarithm of the normalized peak intensities (ln C/C_o) corresponding to MB (red squares) and RhB (black circles). The solid lines are the resulting fits to the data using linear regression.

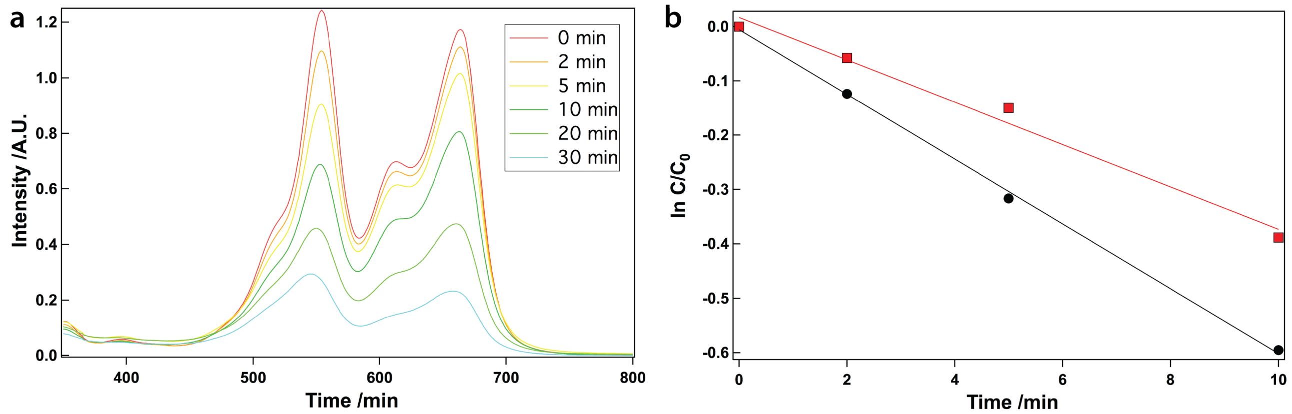

Figure S9. Selective dye degradation in photocatalytic TiO_2NS dispersed in water containing 37.5 mM PDDA. (**a**) UV-vis spectra showing time-dependent changes in the intensity of the spectral features from a mixed solution of Methylene Blue (MB; abs$_{max}$ = 668 nm) and Rhodamine B (RhB; abs$_{max}$ = 555 nm). (**b**) Plots of time-dependent changes in the natural logarithm of the normalized peak intensities (ln C/C_o) corresponding to MB (red squares) and RhB (black circles). The solid lines are the resulting fits to the data using linear regression.

SI TABLES

Table S1. Exponential decay constants (λ) determined for the photocatalytic degradation of various dye molecules in the presence of TiO_2NS-containing coacervate micro-droplets

	λ_{Mb} /min^{-1}	λ_{RhB} /min^{-1}	λ_{X3B} /min^{-1}	λ_{SRhB} /min^{-1}
TiO_2NS/PDDA /KPSE	0.094 (6)	0.030 (3)	0.072 (2)	0.018 (1)
TiO_2NS/PDDA /KPSE (+ NaCl)	0.137 (5)	0.060 (5)	0.106 (6)	0.032 (3)
TiO_2NS/PDDA /ATP	0.0310 (5)	0.004 (1)	0.020 (1)	0.003 (2)
TiO_2NS/PDDA /ATP(+ NaCl)	0.036 (1)	0.005 (1)	0.018 (1)	0.0042 (5)
TiO_2NS/water	0.49 (2)	0.331 (6)	0.117 (3)	0.24 (1)

Table S2 Simulated number of charges on the dye molecules in the pH range of 7-8.

	MB	RhB	X-3B	SRhB
Cationic sites	1	1	0	1
Anionic sites	0	1	2	2

Table S3. Catalytic efficiencies (**Λ**) showing the effect of TiO_2NS concentration on the photocatalytic dye degradation of Methylene Blue (MB) for TiO_2NS dispersed in water, in the PDDA/KPSE bulk coacervate phase, and in PDDA/KPSE coacervate microdroplets.

[TiO_2NS] /mg.mL^{-1}	Λ_{Water} /min^{-1}mg^{-1}	$\Lambda_{PDDA\text{-}KPSE\ bulk}$ /min^{-1}mg^{-1}	$\Lambda_{PDDA\text{-}KPSE\ droplets}$ /min^{-1}mg^{-1}
0.05	0.56 (1)	0.060 (4)	0.13 (1)
0.125	0.61 (7)	0.095 (5)	0.138 (6)
2.5	0.34 (1)	0.028 (1)	0.098 (3)

Table S4. Zeta potential (ζ-V) and hydrodynamic diameters (d_{hyd}) of TiO_2NS in different media.

	H_2O	PDDA	ATP	KPSE
ζ-V /mV	+26.2	+52.7	-34.1	-29.7
d_{hyd} /nm	270 ± 10	1620 ± 25	570 ± 130	440 ± 10